FOREX Publication
Open Access | Rapid and quality publishing

International Journal of
Electrical and Electronics Research (IJEER)
Research Article | Volume 11, Issue 2 | Pages 401-411 | e-ISSN: 2347-470X

A Fractional Order Tilt Integral Controller Based Load Frequency Control with Dispersed Generation and Electric Vehicle

T. Dinesh[1*] and M. Manjula[2]
[1]*Department of Electrical Engineering, Osmania University, Hyderabad, Telangana, India; dinuferrari03@gmail.com*
[2]*Department of Electrical Engineering, Osmania University, Hyderabad, Telangana, India; manjulagooga@gmail.com*

***Correspondence:** T. Dinesh; dinuferrari03@gmail.com

ABSTRACT- The elevated level of entrance of decentralized power sources with their Intermittent and volatility gives us a accost task to control load frequency, moreover this quandary is getting worsen up with the Involvement of electric vehicles in the rundown. This paper presents a censorious robust fractional order operative established tilt integral derivative controller (FOTID) for regulating the frequency. To emulate distributed power sources a linearized model of a wind power plant is considered and a small signal model of EV is developed. With the consideration dynamic nature of EV & wind power plants, the dynamic pursuance of the envisaged FOTID controller is investigated by comparing them with integral order PID controller, Fractional order PID controller, sliding mode controller under various conditions. The transfer function model of proposed controllers is derived and the robustness of the proposed FOTID controller is examined by conducting detailed simulation studies.

Keywords: Load frequency control, Multi area power systems, FOC (Fractional order control), IOC (Integral order control) TID (Tilt angle Derivative), EV (Electric Vehicle), TPP (Thermal Power plant), SMC (Sliding Mode Control).

ARTICLE INFORMATION
Author(s): T. Dinesh and M. Manjula;
Received: 10/04/2023; **Accepted**: 01/06/2023; **Published**: 15/06/2023;
e-ISSN: 2347-470X;
Paper Id: IJEER 1004-05;
Citation: 10.37391/IJEER.110221
Webpage-link:
https://ijeer.forexjournal.co.in/archive/volume-11/ijeer-110221.html

Publisher's Note: FOREX Publication stays neutral with regard to Jurisdictional claims in Published maps and institutional affiliations.

1. INTRODUCTION

The fundamental goal of electrical power system is to maintain the balance between total power output and total demand including losses. It is the responsibility of auxiliary controller to control the load Frequency depending on optimal value to assure the trait of the power supply [1-2]. This process of stabilizing the frequency is called load frequency control. According to [3-4] it is the most significant control challenge in power system design & operation. Authors in [3-4] also discussed that the role of LFC is to maintain zero steady state error for frequency, reducing the number of unplanned power transfers between adjacent control zones, maintaining solid handle on load needs and disruptions, minimizing overshoot and settling time on interconnecting power frequency.

Global attention has been drawn to environmental issues such as increasing carbon emissions due to fast growth of economy, carbon dioxide emission are caused by the burning of fossil fuels for generating power. For carbon free power generation huge intermittent non-conventional energy is already being incorporated into power system networks globally [5-6]. Over time, the usage of green energy has become more wide spread as a means of reducing the energy shortages. In recent years, advancement in technology has allowed wind forms to create more electrical energy. When it comes to generating electricity for its customers, power industry is investing more on wind power. Wind mills are now being integrated in to the actual power system in order to extend grid connectivity. However due to frequency variations, the wind mills connected to current electricity grid gives certain problems. The major concerns in operating wind power plants are issues in MPPT, synchronizing problems, complexity in parameter calculation [7-9]. Grid integrated wind mills must meet the same LFC requirements as traditional power stations under any circumstances. There are several research gaps devoted to the combination of wind and thermal power in hybrid power system [10].

In present situation, the number of EVs has steadily increased and they have become a significant burden on the power grid, which cannot be neglected. It is known that EVs and the power grid encounter in a complex way, for example in [11,12] the design of EV and their involvement in frequency control is discussed. The addition advantage obtained by deploying V2G application is economical by enabling bidirectional power flow [11]. Increasing in uncertainty in load demands and incorporation of dispersed power sources causing huge frequency variations in the system. This laid the researches to concentrate on putting EVs to regulate the frequency [13-14] However wind mills & EVs interconnection to grid is suffering from major problems like, frequency instability due to low inertia system and dynamic charging discharging of electric vehicles. Traditionally the normal LFC system is also suffering from non-linearity, load disturbances, mismatch uncertainty.

The control approaches have been utilized for LFC discussed in [15-18] lacking from system parameters uncertainty is

FOREX Publication
Open Access | Rapid and quality publishing
International Journal of Electrical and Electronics Research (IJEER)
Research Article | Volume 11, Issue 2 | Pages 401-411 | e-ISSN: 2347-470X

becoming more and more prevalent. Power system models are estimated as linear models around an operational point in traditional LFC design, without addressing generator dynamics. For years, PID control has been widely used as a general frequency control approach. A simple design and implementation of PID controller [19-21] makes easy to use, but the performance of their controllers are efficient under fixed power system parameters, but when the system parameters changes then such traditional controllers will fail to trace the output.

Under these situations it is important to implement the controllers which are tenacious and adaptable [22-23]. A fraction order controller is therefore a new idea where the basic principle in this control structure is to expand integer order terms of integration which is differentiating the fractional order operator. So, these control law has more degrees of freedom when compared with integral order control. Hence, fractional controller can achieve good performance in perspective of low settle seek and $\%M_p$ than IOC. In [24-25] FOC is implemented but direct implementation of FOC is not straight forward and it is also evident that selection of λ is much sensitive and sometime under dynamic situation it leads to instability. This problem can be solved using a sliding mode control (SMC) method. We choose it as a result of its ability to withstand load disruptions and parameter changes. The criteria described in [26-27] were used to build the SMC scheme for LFC in interconnected power system.

However, in order to remove the matching external disruption signal, the sliding mode control will come across chattering problem which is not addressed in above literature. The linear model of two area system with EVs and wind power plant is presented in paper. This paper presents a new fractional order tilt integral control of LFC for multi area system. This controller has benefits of TID and FOPID. The results obtained from FOTID are compared with PID, FOPID and SMC controllers in terms of Settling time, peak overshoot, number of peaks, the final results have proved the effectiveness and sensitivity of controller gains towards parameter variations.

2. CONFIGURATION OF PROPOSED SYSTEM

The above *figure 1* shows the abridged model of grid connected system which consist of conventional thermal power plant dispersed generation like wind power plant, EVs and stepped loads. In conventional power grids the frequency control mainly depends on equivalence between power generated and demand. In case any imbalance occurs the control of frequency can be done in three different ways first one is primary control in which frequency control achieved by various speed regulation constant. In secondary control an auxiliary controllers is employed to stabilize the frequency, finally in inertia control the inertia offered by synchronous generator will take care of speed according to change in power demand [28]. This explains us clearly that the dispersed generating systems which involve in regular grid connected system must have inertia, so from *figure 1* the EVs which involving in the system is accompanied with inertia.

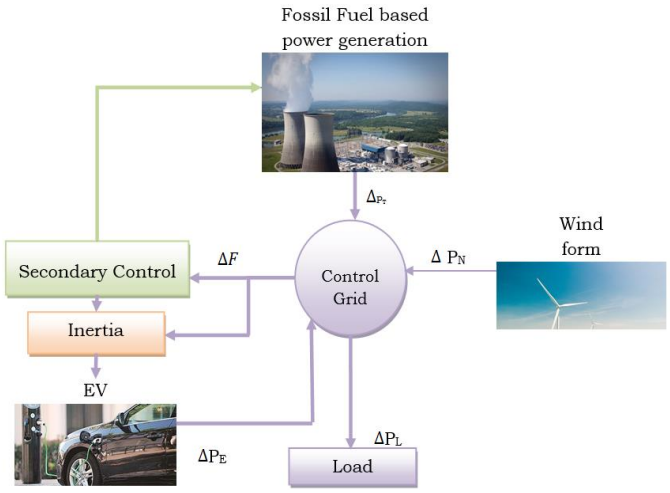

Figure 1: Configuration of proposed system

The governing equation for frequency control in the i^{th} area;

$$\Delta P_{Ti} + \Delta P_{Hi} \pm \Delta P_{EVI} - \Delta P_{Li} - \Delta P_{Tiei} = \Delta f_i(2H_{gi} = D_{gi}) \quad (1)$$

Where,
ΔP_{Ti} = Turbine Output Power
ΔP_{wi} = Generator Electrical Output
ΔP_{EVi} = Electrical Vehicle output power
ΔP_{Li} = Electrical Load Demand
ΔP_{Tiei} = Tie Line Power
Δf_i = Change in frequency in area 1
H_{gi} = Inertia Constant
D_{gi} = Damping Constant

3. SMALL SIGNAL MODELING INVESTIGATED SYSTEM

The power system under consideration in this article is a multi-area linked network with conventional TPP, a wind turbine generator and inertia based electric vehicle in both the areas. A tie-line connects both the locations for power exchange. *Figure 2* depicts the small signal model of proposed system in which total installed capacity of 3000MW and 1500MW load in individual area. Assumed base power is 1000MVA.

FOREX Publication
Open Access | Rapid and quality publishing
International Journal of Electrical and Electronics Research (IJEER)
Research Article | Volume 11, Issue 2 | Pages 401-411 | e-ISSN: 2347-470X

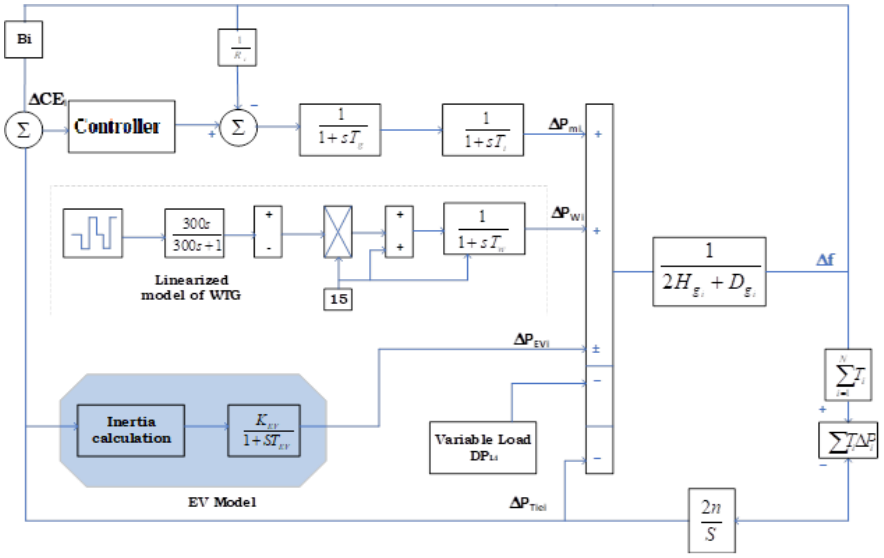

Figure 2: Small signal model of envisaged system

3.1 Modeling of Electric Vehicle

In conventional power system frequency control is based on the balance between generated power and load. Where as in the event of frequency variation caused by a power imbalance the alternators automatically accelerate/decelerate in line with the actual frequency. In simple words the kinetic energy (KE) stored in rotational mass of alternator will regulating the imbalanced power between generation load and so maintain frequency within the limits through this action. However, in current electric grids, inclusion of dispersed generating systems can considerably reduce the total system inertia owing to lack of rotating mass [29]. The stability and dependability will be jeopardized when inertia decreases.

By investigating the inertia-based power response in traditional systems which are generally accommodated by KE of rotating mass. The KE of rotating mass and rotating load is represented as

$$E_{Ke} = \frac{1}{2} J w^2 \tag{2}$$

J = Moment of Inertia (kg/m^2)
ω = angular frequency (rad/sec)

From the dynamics of rotor of generator, the inertia constant (H) defined as ratio of KE to base power [30]

$$H_g = \frac{E_{KE}}{S_b} = \frac{JW^2}{2sb} \tag{3}$$

Where S_b = base complex power

The behavior of rotor of alternator can be easily explained by swing equation

$$\Delta P_m - \Delta P_L = \underbrace{2H_g s\Delta f}_{\Delta P_{Hg}} + \underbrace{D_g \Delta f}_{\Delta P_{Dg}} \tag{4}$$

From *equation (4)* it is evident that the inertia power mainly depends on the time derivative of frequency [31]. As a result to mimic the inertia in RES the first derivative of frequency must be estimated. This concept of derivative of frequency will emulate a change in overall inertia, eventually it will stabilize the frequency in low inertia system. Mathematically it can be represented as

$$\Delta P_{mimiced} = H_{ev} \frac{d\Delta F}{dt} + D_{ev}\Delta f$$
$$\Delta P_{mimiced} = H_{ev} S\Delta f + D_{ev}\Delta f \tag{5}$$

Where H_{ev} and D_{ev} are EV inertia and damping constant.

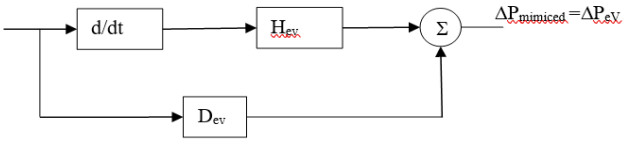

Figure 3: Block Diagram of EV Model

Figure 3 shows EV mode with inertia, however the major concern is with the frequency measuring devices which will create noise while measuring hence a low pass filter is deployed to minimize the effect of noise then,

$$\Delta P_{EV} = \frac{1}{1+ST_e} + \Delta P_{mimiced}$$
$$\Delta P_{EV} = \frac{1}{1+ST_e}[(H_{ev}S + D_{EV})\Delta F] \tag{6}$$

3.2 Modeling of Wind Turbine

Mathematically the power generated from wind turbine generator is given as [32]

$$P_N = \frac{V^3 C_P A_p \rho}{2} \tag{7}$$

Where *Cp* is rotor blades power coefficient, *Ap* is area rotor boomed area, ρ is the density of air, V is the velocity of wind.

FOREX Publication
Open Access | Rapid and quality publishing
International Journal of Electrical and Electronics Research (IJEER)
Research Article | Volume 11, Issue 2 | Pages 401-411 | e-ISSN: 2347-470X

However, the power coefficient of rotor blades is complete dependent of pitch angle $C\beta$, and tip speed ration λ, mathematically it can be expressed as

$$C_p = \frac{\sin((\lambda-2)\Pi)}{(0.3\beta-15)}(0.0167\beta - 0.44) - \beta(\lambda-3).0184 \quad (8)$$

Where $\lambda = \frac{\omega_b R}{V}$ ω_b are speed of blade and R is radius of rotor The torque of wind turbine generator (HTG) is given as $T_N = \frac{P_W}{\omega_b}$ Where, $\omega_b = \frac{\lambda}{R}$

$$T_w = \frac{C_P A_p \rho R^3}{R} \quad (9)$$

When T_w is applied the wind turbine wire revolve at the rate with ω_b. Assuming that T_g & T_L are the generator torques applied by gear box torque and load torques, the shaft of generator wire also revolve at ω_r [34]. There are few equations that are often used to describe turbine and generator dynamics

$$T_w - T_m = J_r\ddot{\theta_r} + D_r\dot{\theta_r} + K_r\theta_r \quad (10)$$
$$T_p - T_e = J_s\ddot{\theta_s} + D_s\dot{\theta_s} + K_s\theta_s \quad (11)$$
$$T_p\dot{\theta_s} = J_M\dot{\theta_r}$$

Where J_1 D & K are inertia constant damping constant & shaft stiffness facts and r, s indicates stator and rotor subscripts [33] As per swing equation we can write

$$T_a - T_g = J_r\ddot{\theta_r} + D_r\dot{\theta_r} + K_r\theta_r \quad (12)$$

If $T_a - T_g = C$ then equation (17) can be written as

$$C = J_r\ddot{\theta_r} + D_r\dot{\theta_r} + K_r\theta_r \quad (13)$$

The transfer function of wind turbine system can be given as

$$G_N(s) = \frac{P_N(s)}{C(s)} = \frac{T_g s}{J_t s^2 C_t s + K_t} \quad (14)$$

In this paper generate time constant (Tg) is considered as constant than $P_w = T_g\omega_r$ so the output power can be controlled by wind speed (ω_b)

3.3 Mathematical Model of Fractional Order Control

It is essential to know the fractional order calculus prior to define the FOPID controller. Those certain operators' mathematical information is available here included in [34–36]. Introduction to obtain FO calculus is described below. To consummate control of MFGII with help of fractional integral sliding surface FSMC is designated later.

$$h^{B\alpha}_s = \begin{cases} \frac{d^\alpha}{ds^\alpha}, R(\alpha) > 0 \\ 1, R(\alpha) = 0 \\ \int_h^s (dT)^{-\alpha}, R(\alpha) < 0 \end{cases} \quad (15)$$

In above expression 'B' represents the fractional calculus operator 'α' denotes fractional order which may be a complex (or) real numbers extremes of operation are expressed by h and s real part of 'α' is expressed by R(α). FOPID controller is in transfer function form can be written as

$$PI^\lambda D^\mu = k_p + \frac{k_I}{s^\lambda} + K_d s^\mu \quad (16)$$

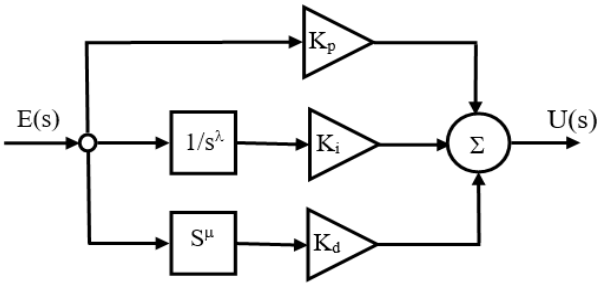

Figure 4: Schematic diagram of FOPID Controller

Figure 4 shows the block diagram of FOPID controller, where k_I, k_p, k_D are the variable integral, proportional, and differential gains λ and μ are adjustable fractional order operators within the range of (0,1)

3.4 Mathematical model of TID Controller

The TID controller's tilt component is derived from non - integer order calculus, whereas the FOPID controller's integral and derivative terms are derived from non - integer order operators. FOPID and TID controllers have high amounts of flexibility than IOCs. As a result, they can increase the effectiveness of control systems which are linked with a broad range of dynamics. In this two-region, there is one Tilted integral derivative controller per area (TID). When running in a wide range of conditions, a traditional PID controller with fixed gains will fail [37-39]. As a result, researchers consider using a TID controller to improve a system's performance standards. TID's proportional element is replaced by a Tilted element, which is identical with that of a Conventional PID controller. Tilted components are represented using Fractional Integrators, such as $1/s^{(1/n)}$ for example. This controller differs from others in that it has a simple design approach and can be tuned quickly and easily.

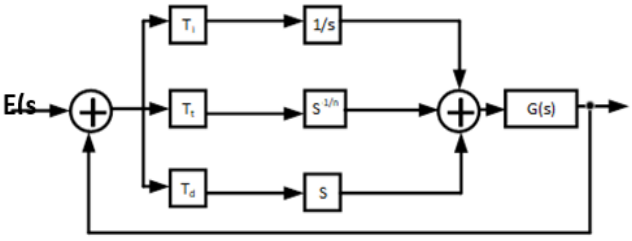

Figure 5: Schematic diagram of FOTID Controller

Here K_P, K_D, K_I denote proportional gain, derivative gain, and integral gain, and n denotes a non-zero real number. Tilted element is registered in such a way that it imbues a frequency feedback gain that concocts itself in relation to the frequency of a traditional recompense unit.

TID controller is now in transfer function model is written as

FOREX Publication
Open Access | Rapid and quality publishing
International Journal of Electrical and Electronics Research (IJEER)
Research Article | Volume 11, Issue 2 | Pages 401-411 | e-ISSN: 2347-470X

$$TID(s) = k_T s^{(-1/n)} + \frac{k_I}{s} + K_D s \quad (17)$$

Figure 5 Shows Schematic diagram of FOTID Controller, Where K_I, K_T, and K_D all refer to three changeable variables defined as the integral, tilt and derivative gains. This work consistently uses n = 3 throughout. Another n value produces a somewhat different outcome.

4. FOTID CONTROLLER GAIN CALCULATION USING INTEGRAL ERROR METHOD

The control design of FOPID controller using integral error method is explained. The main objective is to calculate controller gains like k_P, k_I, λ and μ at constant k_D. This work uses non-reheat turbine of first order is used and the gains used are $k_p = k_I = k_D$ T_g, T_I, T_L, R. The Controller transfer function c(s) is given as

$$C(s) = k_p + \frac{k_I}{S^\lambda} + K_D s^\mu \quad (18)$$

Now the characteristic equations are given by
1+G(s)C(s) = 0

$$1 + \left[k_p + \frac{k_I}{s^\mu} + k_D s^\mu\right] * G(s) = 0 \quad (19)$$

$$(s) = \frac{k_p}{(T_p s+1)(T_T s+1)(T_g s+1)+\frac{k_p}{R}} \quad (20)$$

$$G(s) = \frac{250}{s^3+15.88s^2+42.46+106.2} \quad (21)$$

$$G(s) = 1 + \left(\frac{250}{s^3+15.88s^2+42.46+106.2}\right)\left(k_p + \frac{k_I}{s^\mu} + k_D s^\mu\right) \quad (22)$$

$$R(s_1 k_p, k_I, k_D, \lambda, \mu) = s^{3+\lambda} + 15.88s^{2+\lambda} + 42.46s^{1+\lambda} + \left(106.2 + 250k_d s^{\lambda+\mu} + 250k_I\right) = 0 \quad (23)$$

The system will converge when the roots of eq. (23) lies on the left half of s-plane. But the roots calculated from eq. (23) will has real roots and complex roots. However, a boundary can be formed after calculation, but system will converge only if real boundary intersects with complex boundary

RB = R(s, k_p, k_I, k_D, λ,μ) = 0 for ω ∈ (0,∞),CB = R(s, k_p, k_I, k_D, λ,μ) = 0 for u ∈ (0, ∞).To get real boundary (RB) sub s = 0 then k_I = 0 and to obtain complex boundary (CB) sub s = jω

$$H(s_1 k_p, k_I, k_D, \lambda, \mu) = (j\omega)^{3+\lambda} + 15.88(j\omega)^{2+\lambda} + 42.46(j\omega)^{1+\lambda} + \left(106.2 + 250k_p\right)(j\omega)^\lambda + 250k_d(j\omega)^{\lambda+\mu}\big) + 250k_I\big) = 0 \quad (24)$$

We know

$$j^\lambda = cos\frac{\lambda\pi}{2} + jsin\frac{\lambda\pi}{2}$$

Then, we will get

$$H(\omega, k_p, k_I, k_D, \lambda, \mu) = Re + JIm$$

$$Re = \left[\omega^{3+\lambda} - 42.4w^{1+\lambda}\right]sin\frac{\lambda\pi}{2} + \left[\left(106.2 + 250k_p\right)\omega^\lambda - 15.88w^{2+\lambda}\right]cos\frac{\lambda\pi}{2} + 250k_d\omega^{\mu+\lambda}cos\frac{(\mu+\lambda)\pi}{2} + 250k_i \quad (25)$$

$$jIm = j\left[\left(42.4w^{1+\lambda}\right) - \omega^{3+\lambda}\right]cos\frac{\lambda\pi}{2} + \left[\left(106.2 + 250k_p\right)\omega^\lambda - 15.88w^{2+\lambda}\right]sin\frac{\lambda\pi}{2} + 250k_d\omega^{\mu+\lambda}sin\frac{(\mu+\lambda)\pi}{2} \quad (26)$$

To obtain the value of k_p, k_i & k_D it is required to assume k_D any arbitrary value and then solve eq.(25) and eq.(26) for boundaries λ €(0,1), μ€(0,1). Here in this way we have fixed k_d = 0.84 and then need to solve eq.(25) and eq.(26).These two equations are completely depending on the λ & μ value so if λ, & μ is varied between (0-1) and ω = (0 - ∞) the curve k_p Vs k_I is called complex boundary. The intersection obtained from CB & RB is called global stability. For largest stability margin λ & μ are varied between (0-1) to get many k_p & k_I values. The optimized values of k_p = 2 k_I = 3 are obtained at λ = 0.005, μ = 0.8 which is done on the basis of integral area method

$$C(s) = 2 + \frac{3}{s^{0.005}} + 0.84s^{0.8}$$

4.1 FOTID Controller Gain Calculation Using Integral Error Method

The control design of FOTID controller using integral error method is explained. The main objective is to calculate controller gain like k_T, k_I, λ and μ at constant k_D is to be calculated. The stability investigation is done by using frequency response analysis is also carried out in this section. Controller transfer function c(s) is given as $TID(s) = K_T s^{(-1/n)} + \frac{K_I}{s} + K_D s$ and plant transfer function is given by $G(s) = \frac{250}{s^3 + 15.88s^2 + 42.46 + 106.2}$

Now the characteristic equations are given by
1+G(s)C(s) = 0

$$1 + \left(k_T + \frac{k_I}{s^n} + k_D s\right)\left(\frac{250}{s^3+15.88s^2+42.46+106.2}\right) \quad (27)$$

$$1 + \frac{(K_T s^n + K_I + K_D s^{n+1}) * 250}{s^n(s^3+15.8s^2+42465+106.2)} = 0 \quad (28)$$

$$S^{n+3} + 15.8s^{n+2} + 42.46s^{n+1} + 106.2s^n + 250K_T s^n + 250K_I + 250K_D S^{n+1} \quad (29)$$

Similarly, to RB sub s = 0, K_I = 0 and to get complex boundary sub s = Jω

$$Re = [15.8\omega^{n+2} + (106.2 + 250K_T)\omega^n]cos\frac{n\pi}{2} - [42.46\omega^{n+1} + 250k_d\omega^{n+1}]sin\frac{\pi n}{2} + 250k_I \quad (30)$$

$$jIm = +j\left\{[106.2 + 250K_T]\omega^n sin\frac{n\pi}{2} - \omega^{n+3}\right\} \quad (31)$$

To obtain K_I & K_D as earlier discussed assuming any K_D arbitrary value and then solving eq. (30) & eq. (31) for n∈(0,3). According to integral area method the system is converging and even giving many gains (K_p & K_I) at n = 2 & 3

FOREX Publication
Open Access | Rapid and quality publishing
International Journal of Electrical and Electronics Research (IJEER)
Research Article | Volume 11, Issue 2 | Pages 401-411 | e-ISSN: 2347-470X

$$C(s) = \frac{K_T}{(S^{1/3})} + \frac{K_I}{s} + K_D s \quad (32)$$

5. RESULTS AND DISCUSSION

Case I: Two Area System Without Wind power source and Electric Vehicle (Controlled and Uncontrolled Case with all Proposed Controllers)

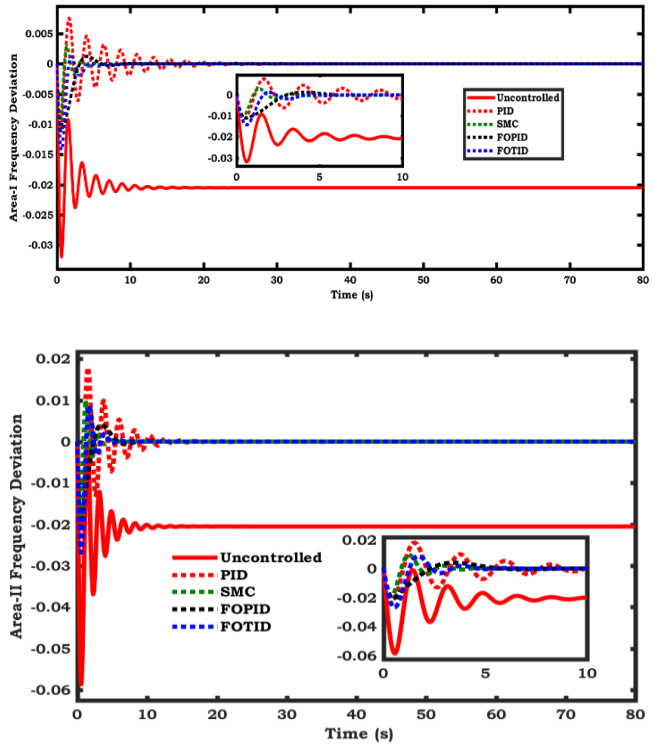

Figure. 6. Frequency deviation of Area-1 & Area-2

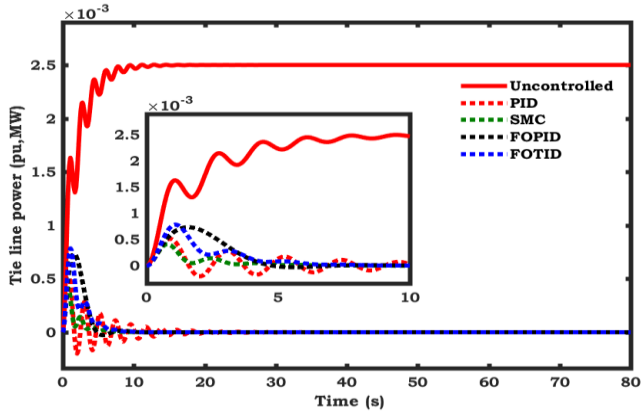

Figure 7: Tie Line Power of two area system in pu, MW

A linked two-area power system can be considered to investigate the dynamic effectiveness of the proposed controller with in AGC loop, Both the areas consist of TPP, wind farm, and Electric Vehicle. To investigate the efficiency of proposed controller the complete simulation studies are carried out for eight different cases and graphical results are presented for all the cases with tabulated Time domain specifications. The pursuance of envisaged controller is compared with PID, SMC and FOPID Controllers. The variable ambiguity is a key concern in today's sophisticated power systems. As a result, it is critical that the control technique used to regulate the LFC be resistant to the system's parameter uncertainties. The power system model is treated as an unpredictable system to examine the resilience of the controller, for this, a 50% minimum and maximum limit uncertainty in plant parameters is assumed, throughout the simulation a step load of 200MW disturbance is applied. Because the major goal of the LFC is to regulate frequency variations in the power system even though the system parameters are not consistent, this characteristic of the FOPID controller makes it extremely appropriate for the LFC.

The results consist of Area-I & II frequency variations and Tie-Line power in pu. The case-I considers Two Area System without Wind power source and Electric Vehicle (Controlled and Uncontrolled Case with all Proposed Controllers) presented in the work. From *figure 7 & 8* it is clearly observed that, using all controllers inside the AGC loop reduces variations in the frequency and tie-line power. Furthermore, within all controllers, the FOTID controller clearly outperforms the others in dampening the oscillations of all signals. *Table 1* compares and lists the dynamic Indices of all signals and controllers, such as Settling time (T_S), percentage Peak overshoot in positive and negative, Undershoot, Number of Peaks and RMS value of signal. From the *table-1* it is very much obvious that the settling time (T_s=7s) obtained for FOPID controller is far much less than the PID, SMC, FOPID controllers. From the *table 1* it is evident that peak overshoot for positive and negative values obtained for FOTID (%M_p = 5.8, -1.9) controller are very less compared to other proposed controllers. This indicates the robustness of proposed FOTID controller. However, the number of peaks (N_p = 2) obtained with proposed controller is less, which indicates the capability of FOTID Controller in damping the frequency oscillations. The RMS value obtained by using FOTID controller is optimal compared to other controllers.

Table-1

Controller	Signal	T_S	M_p %		No. of Peaks	Undershoot	RMS
			+ve	-ve			
PID	Δf_1	24	99	1.90	3	10.6	0.1
	Δf_2	24	141.2	1.965	3	4.46	0.029
	ΔP_{12}	24	60.2	26.02	3	1.99	0.00785
SMC	Δf_1	12	24.37	1.99	3	0.625	0.012
	Δf_2	12	23.6	1.93	3	1.98	0.026
	ΔP_{12}	12	67	15	3	1.98	0.0078
FOPID	Δf_1	10	11.7	1.99	2	2.0	0.00028
	Δf_2	10	11.7	1.99	2	1.99	0.00044
	ΔP_{12}	10	11.7	2	2	1.99	0.1139
FOTID	Δf_1	7	5.8	1.9	2	1.99	0.0006919
	Δf_2	7	13.6	1.99	2	2	0.001094
	ΔP_{12}	7	0.5	1.9	2	1.99	0.1098

FOREX Publication
Open Access | Rapid and quality publishing
International Journal of Electrical and Electronics Research (IJEER)
Research Article | Volume 11, Issue 2 | Pages 401-411 | e-ISSN: 2347-470X

Case: II Two Area System with Wind power source and Thermal power Plant (Controlled case with all Proposed Controllers)

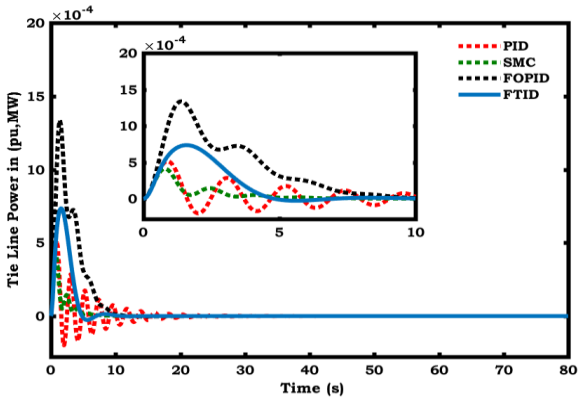

Figure 8: Tie Line Power of two area system in pu, MW

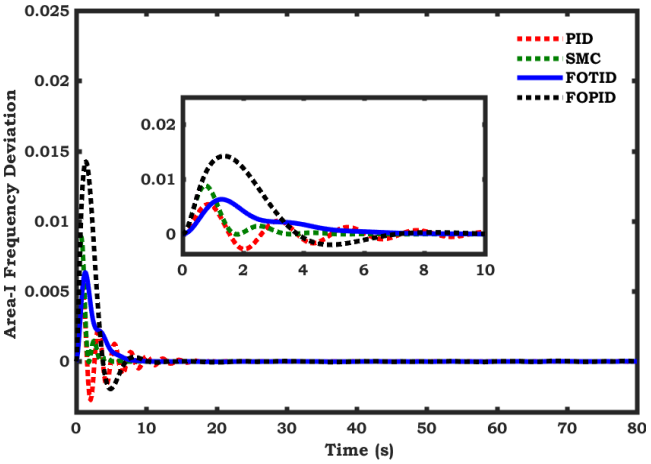

Figure 9: Frequency deviation of Area-1 & Area-2

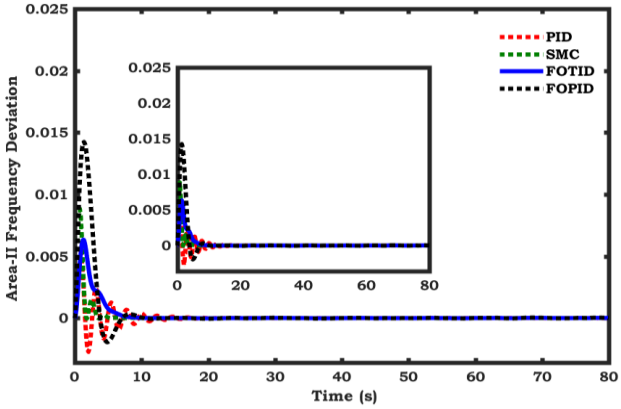

In this case the response of two area system with all controllers by considering the wind mill generating 24MW is presented. The wind mill proposed is not a LFC based power generating system but it is involving in the frequency regulation. From the *figures 8 & 9* it is also clear that the fluctuations obtained are very less with the FOTID controller compared to other controllers. In this case also the settling time offered is 11.1s which is minimum with respect to other controllers. The number of peaks obtained, peak over shoot and RMS value are also optimal in comparison with other controllers which is depicted in *table-2*.

Table 2

Controller	Signal	T_S	M_p %		No. of Peaks	Undershoot	RMS
			+ve	-ve			
PID	Δf_1	18	0.617	27.32	3	1.99	0.01472
	Δf_2	18	0.617	27.3	3	2	0.01472
	ΔP_{12}	18	62.87	25.14	3	1.98	0.07602
SMC	Δf_1	14	0.505	3.5	2	1.99	0.01496
	Δf_2	14	0.505	3.4	2	1.99	0.01496
	ΔP_{12}	14	22.5	1.93	2	1.54	0.03976
FOPID	Δf_1	12.4	0.568	2.2	2	1.9	0.02057
	Δf_2	12.4	0.568	2.26	2	1.9	0.02057
	ΔP_{12}	12.4	0.521	1.9	2	1.98	0.01134
FOTID	Δf_1	11.1	0.562	2.81	2	1.99	0.05098
	Δf_2	11.1	0.562	2.17	2	1.99	0.05097
	ΔP_{12}	11.1	0.515	2	2	1.99	0.01124

FOREX Publication
Open Access | Rapid and quality publishing
International Journal of Electrical and Electronics Research (IJEER)
Research Article | Volume 11, Issue 2 | Pages 401-411 | e-ISSN: 2347-470X

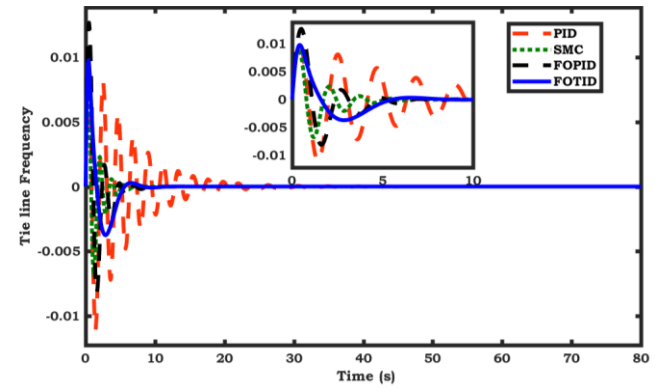

(a)

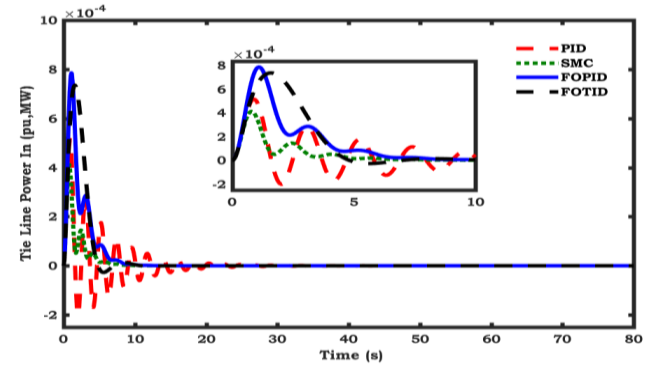

(b)

Figure 10 (a) & (b): Tie Line frequency & power

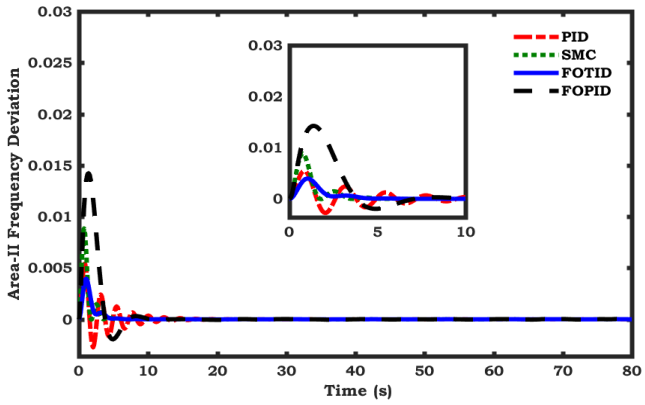

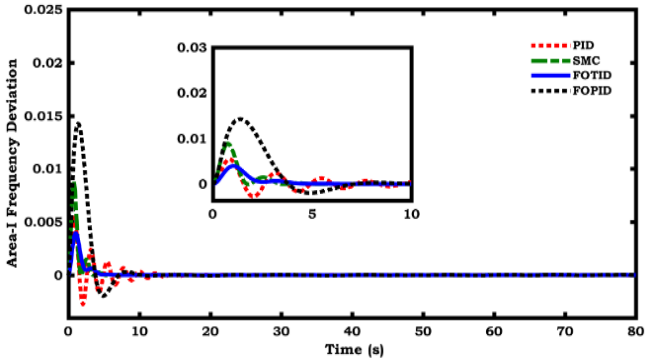

Figure 11: Frequency deviation of Area-1 & Area-2

Table 3

Controller	Signal	T_S	M_P %		No. of Peaks	Undershoot	RMS
			+ve	-ve			
PID	Δf_1	20	0.556	7.21	3	1.99	0.65
	Δf_2	20	0.556	7.23	3	1.997	0.655
	ΔP_{12}	20	1	2.0	3	1.997	0.06634
SMC	Δf_1	15	0.505	3.6	2	0.188	0.72
	Δf_2	15	0.515	3.5	2	1.99	0.726
	ΔP_{12}	15	0.515	3.5	2	1.99	0.0407
FOPID	Δf_1	12	0.575	1.99	2	2.0	0.0002
	Δf_2	12	0.575	1.8	2	1.88	0.0002
	ΔP_{12}	12	0.521	2	2	1.9	0.1139
FOTID	Δf_1	7	0.5	1.2	2	2	0.0497
	Δf_2	7	0.52	2	2	1.7	0.4974
	ΔP_{12}	7	0.51	1.9	2	1.9	0.1098

This case presents two area system with wind mill and electric vehicle participating in the load frequency regulation. The EV model presented in this work is a virtual inertia based electric vehicle model where the virtual inertia is created based on the conventional TPP model. The results obtained in this case is shown in *figure 10 & 11* are clearly indicating the good dynamic efficacy of FOTID controller in terms of time domain indices. *Table-3* shows the complete details of all controllers from that we can justify that FOTID offers settling time, over shoot, number of peaks. In this case particularly FOPID controller also approaching similar response to the FOTID.

FOREX Publication
Open Access | Rapid and quality publishing
International Journal of Electrical and Electronics Research (IJEER)
Research Article | Volume 11, Issue 2 | Pages 401-411 | e-ISSN: 2347-470X

Case: IV Two Area System with 50% Increase in Turbine Time Constant (T_T)

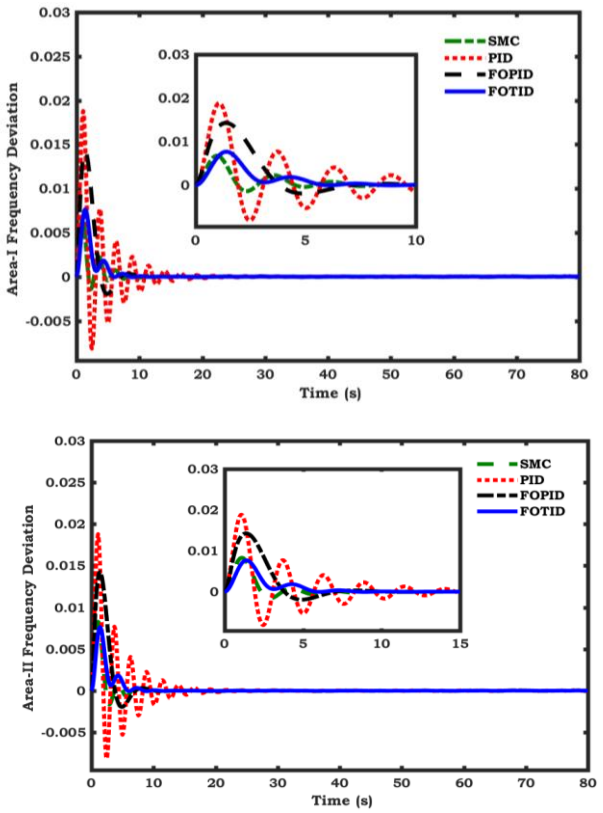

Figure 12: Frequency deviation of Area-1 & Area-2

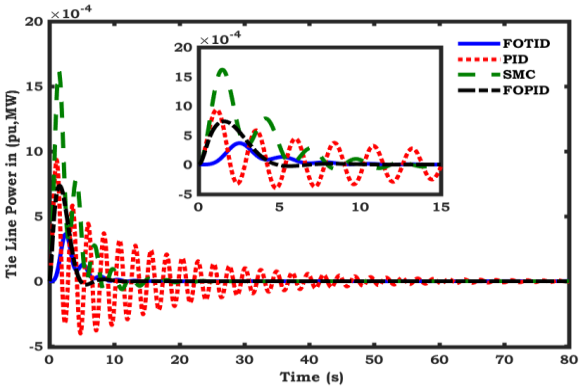

Figure 13: Tie Line power in pu, MW

The sensitivity of FOTID controller towards uncertainties in parameters of power system is considered in this case. Specifically, the turbine constant T_t was considered as 0.4s in the regular model but to create perturbation the turbine time constant is increased by 50% of its original value. Theoretically when turbine time constant is increased then it will reflect in the speed of generator in thermal power plant which directly affects the system frequency, but the proposed robust FOTID controller gains are designed based on the integral error methods is effectively damping out the frequency oscillations, which can be observed from *figures 12 & 13*. From *table - 4* it is evident that the settling time, peak overshot and number of peaks are very less under ambiguity in turbine time constant, which can be also observed from the Table-IV

Table 4

Controller	Signal	T_S	M_p %		No. of Peaks	Undershoot	RMS
			+ve	-ve			
PID	Δf_1	22.7	0.595	27.91	3	1.99	0.02152
	Δf_2	22.7	0.556	13.67	3	2	0.01987
	ΔP_{12}	22.7	116.8	1.98	3	1.98	0.01753
SMC	Δf_1	10.4	0.602	1.2	3	1.99	0.01760
	Δf_2	10.4	0.602	11.6	3	1.98	0.01755
	ΔP_{12}	16.3	124	1.99	3	1.99	0.07232
FOPID	Δf_1	10.2	0.581	2.38	2	1.99	0.02272
	Δf_2	10.2	0.581	2.38	2	1.99	0.02272
	ΔP_{12}	12.2	0.515	2	2	2	0.01205
FOTID	Δf_1	8	0.575	2.5	2	2	0.05644
	Δf_2	8	0.575	2.5	2	2	0.05644
	ΔP_{12}	8	0.515	1.99	2	2	0.01198

FOREX Publication
Open Access | Rapid and quality publishing
International Journal of Electrical and Electronics Research (IJEER)
Research Article | Volume 11, Issue 2 | Pages 401-411 | e-ISSN: 2347-470X

Case V: Two Area System with 50% decrease in Turbine Time Constant (T_T)

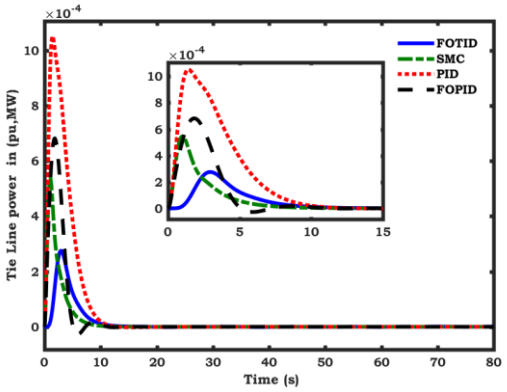

Figure 14: Tie Line power in pu, MW

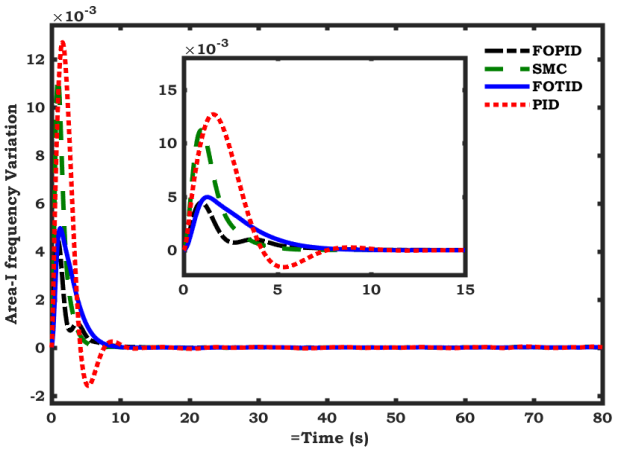

Figure 15: Frequency deviation of Area-1 & Area-2

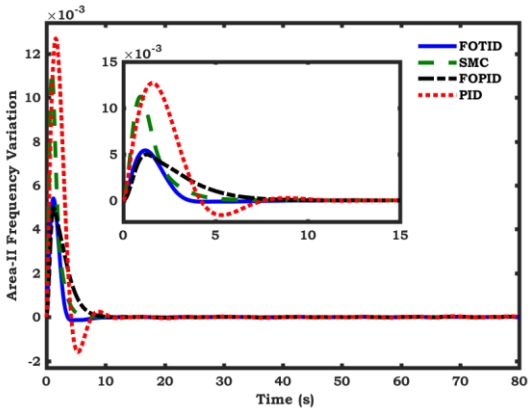

Similar to the case IV the turbine time constant is reduced by 50% to observe the robustness of FOTID controller, *figure 15* clearly shows the difference in the curves for different controllers and *table-5* shows the least settling time obtained is 9s with the proposed controller and the overshoot, undershoot are also very less in the order of 0.562, 2% with FOTID controller. The number of peaks obtained is 2 which is also less.

Table V

Controller	Signal	T_S	M_p %		No. of Peaks	Under shoot	RMS
			+ve	-ve			
PID	Δf_1	14	0.505	2	3	2	0.01111
	Δf_2	14	0.505	2	3	1.99	0.01111
	ΔP_{12}	14	0.505	2	3	1.99	0.05870
SMC	Δf_1	12	0.505	2.7	2	1.99	0.01107
	Δf_2	12	0.505	2.7	2	1.99	0.01107
	ΔP_{12}	12	137.3	1.99	2	1.98	0.02451
FOPID	Δf_1	10	0.52	2.2	2	1.99	0.01920
	Δf_2	10	0.52	2.2	2	1.99	0.01920
	ΔP_{12}	10	0.54	2.4	2	1.99	0.01090
FOTID	Δf_1	9	0.562	2	2	1.99	0.04785
	Δf_2	9	0.562	2	2	1.99	0.04785
	ΔP_{12}	9	0.521	2	2	2	0.01086

6. CONCLUSION

The Drastic increase in load demand and subsequently involvement of distributed power sources like wind, solar power systems in to Conventional grid leads to lot of perturbation in load frequency. This work presents a LFC model which includes Electric vehicles and wind power plant. In this work Fractional order based tilt angle derivative controller is presented for two area system. Furthermore to evaluate the robustness of proposed controller the results are compared with other controllers like PID, SMC & FOPID in terms of settling time, $\%M_p$, number of peaks, Undershoot and RMS value. The values obtained from different controllers are tabulated for easy comparison. From all the tabular data FOTID controller is giving noticeable performance under dynamic conditions. The sensitivity of controller towards parameter uncertainties like (Turbine time constant (T_t), Governor Time constant (T_g), and synchronizing power coefficient is also investigated with all controllers. Finally with clear observation FOTID controller is giving efficient performance with considered complicated model.

FOREX Publication
Open Access | Rapid and quality publishing

International Journal of
Electrical and Electronics Research (IJEER)
Research Article | Volume 11, Issue 2 | Pages 401-411 | e-ISSN: 2347-470X

REFERENCES

[1] Shayeghi H, Shayanfar HA, Jalili A. Load frequency control strategies: a state-of-the-art survey for the researcher. Energy Convers Manage 2009; 50:344–53.

[2] Khodabakhshian A, Ezatabadi Pour M, Hooshmand R. Design of a robust load frequency control using sequential quadratic programming technique. Electr Power Energy Syst 2012; 40:1–8.

[3] Wood Allen J, Wollenberg Bruce F. Power generation operation and control; 1996.

[4] Bevrani H. Robust power system frequency control. Springer; 2009.

[5] Jia Hongjie, Li Xiaomeng, Mu Yunfei, Xu Chen, Jiang Yilang, Yu Xiaodan, et al.Coordinated control for EV aggregators and power plants in frequency regulation considering time-varying delays. Appl Energy 2018; 210:1363-76.

[6] Clairand Jean-Michel, Rodríguez-García Javier, Alvarez-Bel Carlos. Assessment of technical and economic impacts of ev user behavior on EV aggregator smart charging. Journal of Modern Power Systems and Clean Energy 2019; 8(2):356-66.

[7] Van Van Huynh, Bui Le Ngoc Minh, Emmanuel Nduka Amaefule, Anh-Tuan Tran, Phong Thanh Tran,Van-Duc Phan, Viet-Thanh Pham and Tam Minh Nguyen,Load Frequency Control for Multi-Area Power Plants with Integrated Wind Resources,Appl. Sci. 2021, 11, 3051

[8] Aziz A, Oo AT, Stojcevski A. Analysis of frequency sensitive wind plant penetration effect on load frequency control of hybrid power system. Int JElectr Power Energy Syst 2018; 99:603-17.

[9] Liu J, Yao Q, Liu Y, et al. Wind farm primary frequency control strategy based on wind & thermal power joint control. Proc CSEE 2017; 37:3462-9.

[10] Darabian M, Jalilvand A. A power control strategy to improve power system stability in the presence of wind farms using FACTS devices and predictive control. Int J Electr Power Energy Syst 2017; 85:50-66.

[11] Fan Hua, Jiang Lin, Zhang Chuan-Ke, Mao Chengxiong. Frequency regulation ofmulti-area power systems with plug-in electric vehicles considering communication delays. IET Gener, Transm Distrib 2016; 10(14):3481-91.

[12] Liu Hui, Hu Zechun, Song Yonghua, Jin Lin. Decentralized vehicle-to-grid control for primary frequency regulation considering charging demands. IEEE Trans Power Syst 2013; 28(3):3480-9.

[13] Khooban MH, Niknam T, Blaabjerg F, et al. A new load frequency control strategy for micro-grids with considering electrical vehicles. Electric Power Syst Res 2017; 143(1):585–98. https://doi.org/10.1016/jepsr.2016.10.57.

[14] Hasanien HM, El-Fergany AA. Salp swarm algorithm-based optimal load frequency control of hybrid renewable power systems with communication delay and excitation cross-coupling effect. Electric Power Syst Res 2019; 176. https://doi.org/10.1016/j.epsr.2019.105938. 105938.

[15] Liu, F.; Li, Y.; Cao, Y.; She, J.; Wu, M. A two-layer active disturbance rejection controller design for load frequency control of interconnected power system. IEEE Trans. Power Syst. 2016, 31, 3320–3321.

[16] Liu, Y.; Lan, Q.; Qian, C.; Qian, W.; Chu, H. Universal finite time observer design and adaptive frequency regulation of hydraulic turbine systems. IET Control Theory Appl. 2016, 10, 363–370.

[17] Sun, Y.; Qiang, H.; Mei, X.; Teng, Y. Modified repetitive learning control with unidirectional control input for uncertain nonlinear systems. Neural Computing. Appl. 2018, 30, 2003–2012.

[18] Chen, H.; Sun, N. Nonlinear control of under-actuated systems subject to both actuated and unactuated state constraints with experimental verification. IEEE Trans. Ind. Electric. 2019, 67, 7702–7714.

[19] Umesh KR, Rabindra KS, Sidhartha P. Design and analysis of differential evolution algorithm based automatic generation control for interconnected power system. Ain Shams Eng 2013; 4:409–21.

[20] Abdel-Magid YL, Dawoud MM. Optimal AGC tuning with genetic algorithms. Electric Power Syst Res 1997; 38:231–8.

[21] Sidhartha P, Banaja M, Hota PK. Hybrid BFOA–PSO algorithm for automatic generation control of linear and nonlinear interconnected power systems. Appl Soft Computing 2013; 13:4718–30.

[22] Arya Y, Kumar N. BFOA-scaled fractional order fuzzy PID controller applied to AGC of multi-area multi-source electric power generating systems. Swarm EvolComput2017; 32:202–18.

[23] Morsali J, Zare K, Hagh MT. Comparative performance evaluation of fractional order controllers in LFC of two-area diverse-unit power system with considering GDB and GRC effects. J Electric Syst Inf Technol 2018;5(3):708–22.

[24] Muwaffaq IA. Load frequency control and automatic generation control using fractional-order controllers. Electric Eng 2010; 91:357–68.

[25] Sanjoy D, Lalit CS, Nidul S. AGC of a multi-area thermal system under deregulated environment using a non-integer controller. Electric Power Syst Res 2013; 95:175–83.

[26] Mi, Y.; Fu, Y.;Wang, C.; Wang, P. Decentralized sliding mode load frequency control for multi-area power systems. IEEE Trans.Power Syst. 2013, 28, 4301–4309.

[27] Onyeka, A.E.; Xing-Gang, Y.; Mao, Z.; Jiang, B.; Zhang, Q. Robust decentralized load frequency control for interconnected time delay power systems using sliding mode techniques. IET Control Theory Appl. 2019, 14, 470–480.

[28] Arya Y, Kumar N. BFOA-scaled fractional order fuzzy PID controller applied to AGC of multi-area multi-source electric power generating systems. Swarm Evol Comput 2017; 32:202–18.

[29] Morsali J, Zare K, Hagh MT. Comparative performance evaluation of fractional order controllers in LFC of two-area diverse-unit power system with considering GDB and GRC effects. J Electr Syst Inf Technol 2018; 5(3):708–22.

[30] Das S. Functoinal FRACTIONAL CALculus. 2nd ed. Springer Berlin Heidelburg; 2011.

[31] Chen YQ, Zhao C, Xue D. Fractional order PID control of a dc-motor with elastic shaft:a case study. In: Proc. of American control conf., Minneapolis, U.S.A.; June 2006.

[32] Sondhi S, Hote YV. Fractional order controller and its applications: a review. In: Proc. of Asia MIC, Phuket, Thailand; April 2012.

[33] N.R. Tummuru, M.K. Mishra, S. Srinivas, An improved current controller for grid connected voltage source converter in microgrid applications, IEEE Trans. Sustain. Energy 6 (2) (2015) 595–605.

[34] T. Ye, N. Dai, C.S. Lam, M.C. Wong, J.M. Guerrero, Analysis, design, and implementation of a quasi-proportional-resonant controller for a multifunctional capacitive-coupling grid-connected inverter, IEEE Trans. Ind.Appl. 52 (5) (2016) 4269–4280.

[35] W. Al-Saedi, S.W. Lachowicz, D. Habibi, O. Bass, Power flow control in grid-connected microgrid operation using particle swarm optimization undervariable load conditions, Int. J. Electr. Power Energy Syst. 49 (2013) 76–85.

[36] Ge Ming, Chiu Min-Sen, Wang QG. Robust PID controller design via LMI approach. J Process Control 2002;12:3–12

[37] Shabani, H., Vahidi, B., and Ebrahimpour, M. A., "Robust PID controller based on imperialist competitive algorithm for load-frequency control of power systems," ISA Trans., Vol. 52, pp. 88–95, 2012.

[38] S. Padhan, R.K. Sahu and S. Panda, "Application of Firefly Algorithm for Load Frequency Control of Multiarea Interconnected Power System,"Electric Power Components and Systems, vol. 42, pp. 1419-1430. 2014.

[39] T Dinesh, Palle Jayabharath Reddy, Thalluru Anil Kumar "A Coordinated V2G Control For LFC of Multi Area Power System With HVDC Link In Deregulated Environment" International Journal of Pure and Applied Mathematics, Vol 120, Issue 6, pp. 567-586.

© 2023 by the T. Dinesh and M. Manjula. Submitted for possible open access publication under the terms and conditions of the Creative Commons Attribution (CC BY) license (http://creativecommons.org/licenses/by/4.0/).